# Journal of Materials Chemistry A

Accepted Manuscript


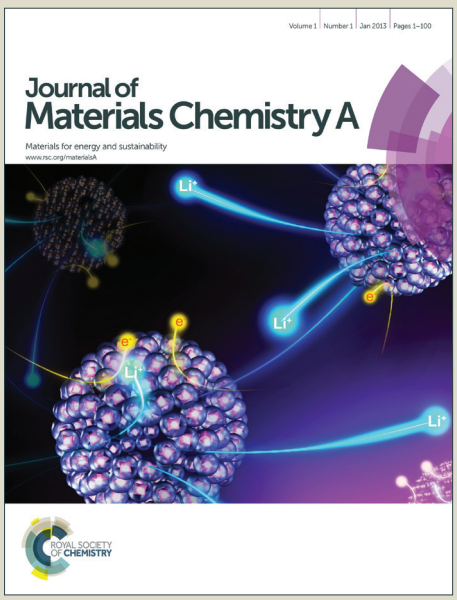



This is an *Accepted Manuscript*, which has been through the Royal Society of Chemistry peer review process and has been accepted for publication.

*Accepted Manuscripts* are published online shortly after acceptance, before technical editing, formatting and proof reading. Using this free service, authors can make their results available to the community, in citable form, before we publish the edited article. We will replace this *Accepted Manuscript* with the edited and formatted *Advance Article* as soon as it is available.

You can find more information about *Accepted Manuscripts* in the Information for Authors.

Please note that technical editing may introduce minor changes to the text and/or graphics, which may alter content. The journal's standard Terms & Conditions and the Ethical guidelines still apply. In no event shall the Royal Society of Chemistry be held responsible for any errors or omissions in this *Accepted Manuscript* or any consequences arising from the use of any information it contains.



ROYAL SOCIETY OF CHEMISTRY

www.rsc.org/materialsA

# Preparation and adsorption performance of cross-linked porous polycarbazoles

Jian-Hua Zhu,[a,b] Qi Chen,[b,*] Zhu-Yin Sui,[b] Long Pan,[b] Jiaguo Yu,[a,*]

Bao-Hang Han[b,*]

[a] *State Key Laboratory of Advanced Technology for Material Synthesis and Processing, Wuhan University of Technology, Wuhan 430070, China*

[b] *National Center for Nanoscience and Technology, Beijing 100190, China*

Tel: +86 10 8254 5576; Email: hanbh@nanoctr.cn

Tel: +86 10 8254 5708; Email: chenq@nanoctr.cn

Tel: +86 27 8787 1029; Email: yujiaguo93@163.com

Journal of Materials Chemistry A Accepted Manuscript

## Abstract

We report a facile method for the preparation of hypercrosslinked carbazole-based porous organic polymers (CPOPs) via $FeCl_3$-promoted one-step oxidative coupling reaction and Friedel–Crafts alkylation in one pot. The Brunauer–Emmett–Teller specific surface area of the obtained polymers is up to 1190 $m^2 g^{-1}$, which is competitive with the reported results for other hypercrosslinked porous polymers. Gas (hydrogen and carbon dioxide) adsorption isotherms show that their hydrogen storage is up to 1.29 wt% at 1.0 bar and 77 K, the uptake capacity for carbon dioxide can reach to 16.8 wt% at 1.0 bar and 273 K, which makes it show promising application in the energy and environment field. Furthermore, the adsorption amount of toluene by **CPOP-15** is high up to 1470 mg $g^{-1}$ (about 16.0 mmol $g^{-1}$) at its saturated vapor pressure and the mass ratio of adsorbed water to toluene is up to 1:7. Meanwhile, the prepared CPOPs possess excellent adsorption capacities for formaldehyde (10.7 mg $g^{-1}$) at ambient condition and exhibit good thermal stability and repeatability at the same time, which makes it show potential application to eliminate harmful small molecules in the environment.


**Keywords:** Adsorption; Friedel–Crafts alkylation; oxidative coupling reaction; hypercrosslinked polymer; porosity; polycarbazoles.

Journal of Materials Chemistry A Accepted Manuscript

## Introduction

Porous polymers with the intrinsic properties including large specific surface areas, high chemical stabilities, and low skeleton density, have exhibited potential applications in heterogeneous catalysis[1, 2, 3, 4] and gas storage[5, 6] and separation.[7, 8, 9] Versatile porous polymers have been obtained smoothly through a template-free chemical process by selection of proper building blocks and polymerization reactions, which show efficient preparation and high flexibility in the molecular design.[10, 11, 12]

Hypercrosslinked porous polymers, as an intrinsic porous organic polymer, represent a family of robust microporous organic materials with good thermal stability, excellent chemical robustness, and relatively low heat of adsorption, which have been used as sorbents for the adsorption of gas and organic vapors and for the removal of organic compounds from water.[13, 14] Friedel–Crafts alkylation reaction is a common method for the preparation of hypercrosslinked porous polymers. Tan's group recently developed a versatile strategy for preparing microporous polymers by a simple one-step Friedel–Crafts alkylation of aromatic monomers using formaldehyde dimethyl acetal (FDA) as an external cross-linker.[15] Through this method, microporous heterocyclic polymers [16, 17] and triphenylphosphine-functionalized hypercrosslinked porous polymers[18] have been successfully prepared for gas uptake and catalyst immobilization, respectively.

Recently, we have reported a facile preparation of porous conjugated polycarbazoles through $FeCl_3$-promoted carbazole-based oxidative coupling polymerization,[19, 20] in



Journal of Materials Chemistry A Accepted Manuscript

which the catalyst $FeCl_3$ can be completely removed after simple workup. Because no other functional groups such as halo group, boric acid, and alkyne are required for coupling polymerization, the effects of reactive group residues need not be considered. Moreover, properties derived from monomers are likely to be fully retained and structures of final polymers are easy to be well characterized.[21] We believe it can be a promising method to facilitate the preparation of porous polymers.

Considering that both Friedel–Crafts alkylation and carbazole-based oxidative coupling reaction can be catalyzed by $FeCl_3$, herein, we prepared a series of hypercrosslinked carbazole-based porous organic polymers (**CPOP-13~15**) via $FeCl_3$-promoted one-step oxidative coupling reaction and Friedel–Crafts alkylation in one pot. Their gas adsorption capacities for hydrogen, carbon dioxide, and methane have been investigated and the related adsorption capabilities for solvent vapors such as toluene, methanol, and water have also been explored. Meanwhile, the obtained carbazole-based porous organic polymers (CPOPs) with high surface area present a good formaldehyde adsorption capacity, which makes it show potential use in elimination of harmful small molecules in the environment.

## Experimental section

**Materials.** Ferric chloride, formaldehyde dimethyl acetal (FDA) and 4, 4'-di(9H-carbazol-9-yl)-1,1'-biphenyl (DCP) were purchased from Acros and Alfa Aesar companies. All chemicals and reagents were used without further purification unless



Journal of Materials Chemistry A Accepted Manuscript

otherwise stated. 1,4-Di(9H-carbazol-9-yl)benzene (DCB) and 1,3,5-tri(9H-carbazol-9-yl)benzene (TCB) were prepared according to reported methods,[19] respectively. The chemical structures of all monomers were fully confirmed.

**Instrumental characterization.** The $^{1}$H NMR spectra were carried out on a Bruker DMX400 NMR spectrometer. Solid-state cross polarization magic angle spinning (CP/MAS) NMR spectra were recorded on a Bruker Avance III 400 NMR spectrometer. Mass spectra were collected by a Microflex LRF MALDI-TOF mass spectrometer (Bruker Daltonics, USA). The infrared (IR) spectra were obtained from a PerkinElmer Spectrum One Fourier transform infrared (FTIR) spectrometer. Thermogravimetric analysis (TGA) was performed on a Pyris Diamond thermogravimetric/differential thermal analyzer by heating the samples at 10 °C min$^{-1}$ to 800 °C in the atmosphere of nitrogen. Gas sorption isotherms were obtained with Micromeritics TriStar II 3020 and Micromeritics ASAP 2020 M+C (Micromeritics Instrument Corporation, USA) accelerated surface area and porosimetry analyzers at certain temperature. The samples were degassed at 120 °C for 12 h under vacuum to remove residual moisture and other trapped gases. The obtained adsorption–desorption isotherms were evaluated to give the pore parameters, including Brunauer–Emmett–Teller (BET) specific surface area, pore size, and pore volume. The pore size distribution (PSD) was calculated from the adsorption branch with the nonlocal density function theory (NLDFT) approach. Total pore volume was calculated from nitrogen adsorption–desorption isotherms at $P/P_0$ = 0.97. The hydrogen sorption isotherm was monitored at 77 K, carbon dioxide and

Journal of Materials Chemistry A Accepted Manuscript

methane sorption isotherms were measured at 273 K and 298 K, respectively. The vapor adsorption–desorption isotherms and high pressure $H_2$ and $CO_2$ physisorption were measured on an IGA-100B intelligent gravimetric analyzer (Hiden Isochema Ltd, UK). The concentration of formaldehyde was on-line analyzed with a Photoacoustic IR Multigas Monitor (INNOVA air Tech Instruments Model 1412, USA).

**Preparation of CPOP-13~15.** 1,4-Di(9H-carbazol-9-yl)benzene (DCB) (82 mg, 0.2 mmol) was dissolved in anhydrous 1,2-dichloroethane (15 mL), and then formaldehyde dimethyl acetal (FDA) (300 μL, 0.2 mmol), ferric chloride (650 mg, 4 mmol) was added to the reaction mixture The mixture was stirred for 1 h under nitrogen at room temperature, and then the mixture was heated to 90 °C and kept at the temperature for 12 h. After the mixture was cooled down to room temperature, 50 mL of methanol was added to the reaction mixture. The resulting mixture was kept stirring for another one hour and the precipitate was collected by filtration. After washed with methanol, the obtained solid was stirred vigorously in hydrochloric acid solution (37 %) for 2 h. The suspension was then filtered and washed with water and methanol. After extracted in a Soxhlet extractor with methanol for 24 h, and then with tetrahydrofuran for another 24 h, the desired polymer **CPOP-13** (yield: 95 %) was collected and dried in vacuum oven at 110 °C overnight. When 4, 4'-di(9H-carbazol-9-yl)-1,1'-biphenyl (DCP) or 1,3,5-tri(9H-carbazol-9-yl)benzene (TCB) was used as the monomer, **CPOP-14** (yield: 92 %) or **CPOP-15** (yield: 96 %) can be obtained according to the same procedure, respectively.



Journal of Materials Chemistry A Accepted Manuscript

**Formaldehyde adsorption test.** Formaldehyde adsorption was measured in an organic glass box covered by a layer of aluminum foil paper on its inner wall at ambient temperature. The experimental setup as shown in Fig. S1 (ESI) was home-made. [22] The adsorbent (0.1 g) was dispersed on the bottom of glass petri dish with a diameter of 14 cm, 25 μL of formaldehyde solution (38 wt%) was injected into the chamber after placing the sample-contained dishes in the bottom of chamber with a glass slide cover. During the whole measurement process, there was a fan (5 W) which sped up the equilibrium of formaldehyde in the bottom of chamber. The formaldehyde solution was volatilized completely and the concentration of formaldehyde was stabilized during 2–3 h. The formaldehyde vapor was allowed to reach adsorption–desorption equilibrium with internal wall of the chamber prior to the adsorption experiment. The initial equilibrium concentration of formaldehyde was controlled at ca.160 ppm, which remained constant until the glass slide cover on the petri dish was removed to start the adsorption of formaldehyde by the porous materials. In the cycling experiments, the adsorbent was heated at 80 °C for 2 h before next run of formaldehyde adsorption.

## Results and discussion

The preparation routes to hypercrosslinked porous polycarbazoles are shown in Scheme 1. Using the aforementioned DCB, DCP, and TCB as monomers and formaldehyde dimethyl acetal (FDA) as the crosslinker, carbazole-based oxidative coupling polymerization and Friedel–Crafts crosslinking polymerization were promoted



Journal of Materials Chemistry A Accepted Manuscript

smoothly by anhydrous $FeCl_3$ in dry 1, 2-dichloroethane under nitrogen atmosphere at 90 °C. This modified method can furnish the desired hypercrosslinked carbazole-based porous organic polymers **CPOP-13**, **CPOP-14**, and **CPOP-15**, respectively. All polymers are stable and insoluble in common solvents as a result of the cross-linking nature.

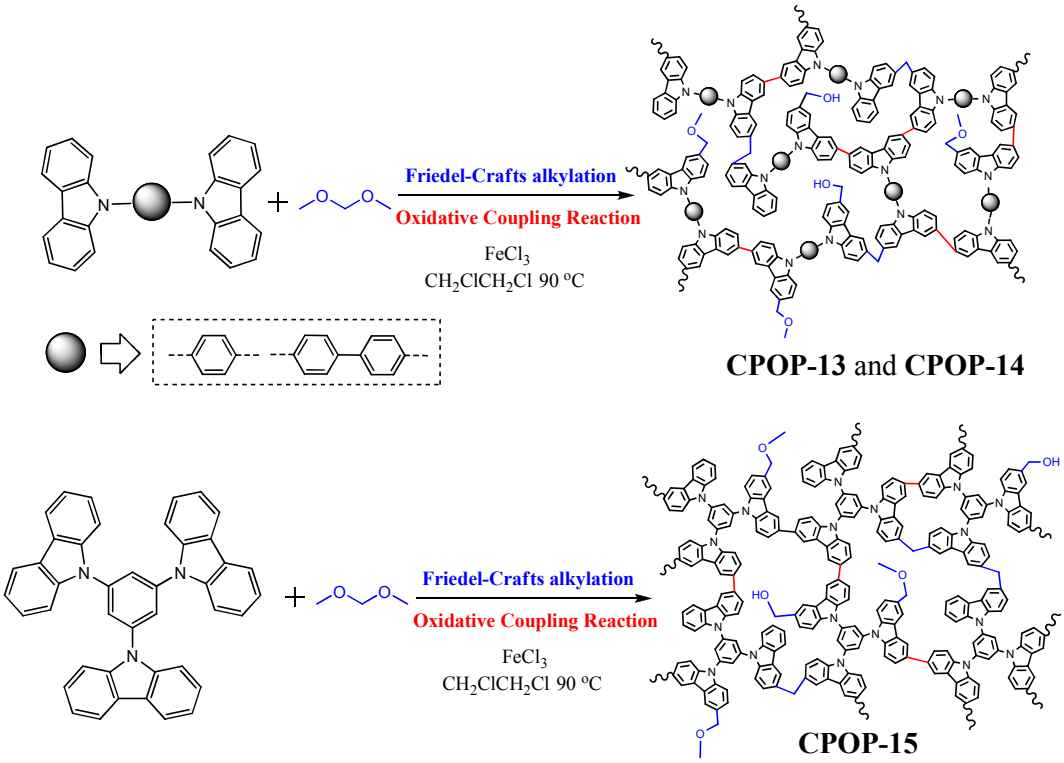


**Scheme 1.** Preparation of hypercrosslinked carbazole-based porous organic polymers (**CPOP-13**, **CPOP-14**, and **CPOP-15**)



Journal of Materials Chemistry A Accepted Manuscript

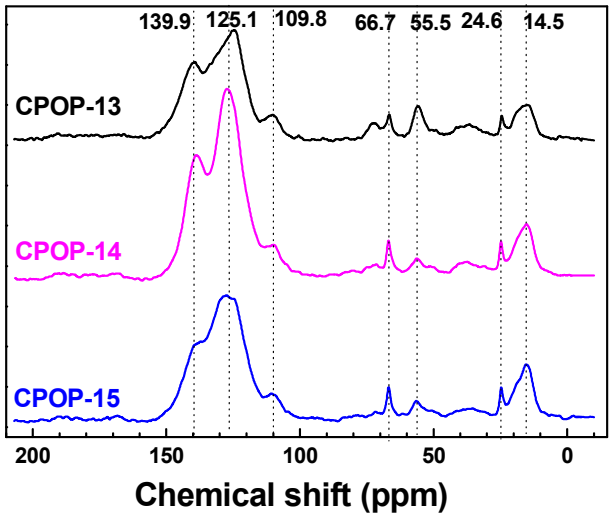


**Fig. 1**. $^{13}$C CP/MAS NMR spectra of **CPOP-13**, **CPOP-14**, and **CPOP-15**.

In order to confirm the successful growth of a microporous polymer, as well as high conversion of the available cross-linker, all polymers were characterized at the molecular level by $^{13}$C CP/MAS NMR spectrum and Fourier transform infrared spectrometer (FTIR). The $^{13}$C NMR spectra for the porous polymers with assignment of the resonances are shown in Fig. 1. Generally, there are three broad peaks approximately at 140−105, 68−55, and 25−15 ppm. For example, for **CPOP-15**, the broad peaks at 140−105 ppm are ascribed to the peak of aromatic carbons. In details, the peak at about 139.9 ppm corresponds to the substituted phenyl carbons binding with nitrogen atom. The high-intensity peak for other substituted phenyl carbons is located at about 125.1 ppm, the signal peak at about 109.8 ppm is ascribed to the unsubstituted phenyl carbons, which are perfectly consistent with the previous work about carbazole based porous organic polymers.[19, 20] It is worth mentioning that the broad peaks at



Journal of Materials Chemistry A Accepted Manuscript

68–55 and 27–15 ppm are newly occurring peaks in contrast with the previous work.[19, 20] The broad peaks at 68–55 ppm are ascribed to the peak of methylene carbons from the linker, the peak at about 66.7 ppm corresponds to methylene carbons binding with oxygen atom, which are ascribed to imperfect reaction of the linker, there are some methylene carbons that just bind with the monomer partially in the materials. Meanwhile, the methylene carbons binding with phenyl, that have reacted with the monomer completely, are located at 55.5 ppm. Furthermore, the broad peaks at 27–15 ppm are ascribed to the peak of methyl carbons peak from the incompletely reacted linker in the tail end.[15, 16]

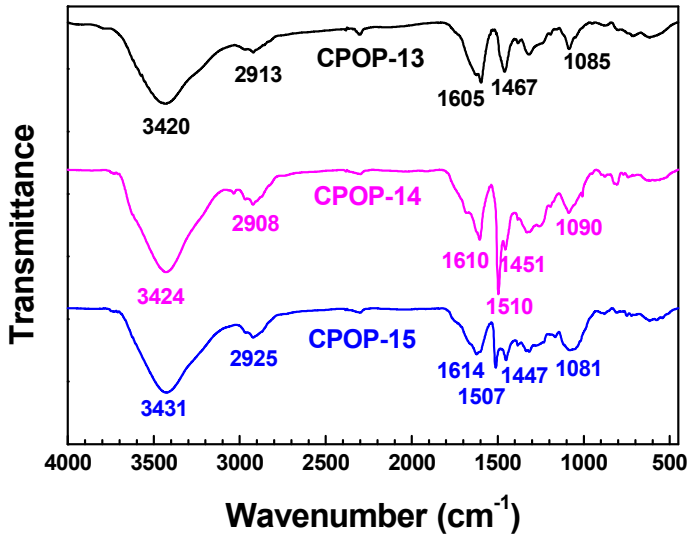


**Fig. 2**. FTIR spectra of **CPOP-13**, **CPOP-14**, and **CPOP-15**.

The structural information of the prepared CPOPs was also obtained by TGA and FTIR spectroscopy. A comparison of the FTIR spectra of the polymer is shown in Fig. 2, in which the peaks at about 1610, 1510, and 1450 $cm^{-1}$ are attributed to aromatic ring



Journal of Materials Chemistry A Accepted Manuscript

skeleton vibrations, which were consistent with the structure of corresponding monomers. In addition, we noticed that the broad absorption peaks at about 3420 $cm^{-1}$ (O–H band stretching vibrations), the weak absorption peaks at about 2910 $cm^{-1}$ (C–H band stretching vibrations) and the peaks at about 1090 $cm^{-1}$ (C–O stretching vibrations) indicate the structure of $–CH_2–$ and a handful of tail end group such as $–CH_2OH$ and $–CH_2OCH_3$ in the hypercrosslinked networks. The FTIR spectra for C–H band stretching of methylene group is also definitely consistent with the result obtained by $^{13}C$ CP/MAS NMR spectra, perfectly consistent with the literature about the hypercrosslinked networks.[15, 16, 23] In conclusion, all the above characterization data can confirm that the linkers have participated in the formation of the cross-linking porous polymers and the desired polymers have been synthesized successfully by carbazole-based oxidative coupling polymerization and Friedel–Crafts crosslinked polymerization.

All polymers are chemically stable, even when exposed to dilute solutions of acid or base, such as HCl or NaOH. The thermal stability of the polymers was characterized by thermogravimetric analysis (Fig. S2, ESI). Mass loss (10%) was observed from 300 to 450 °C under nitrogen, even when the temperature rises to 800 °C, there is only 30% mass loss. It has no evidence for distinct glass transition for these polymers below the thermal decomposition temperature due to the nature of their cross-linking structures.

Journal of Materials Chemistry A Accepted Manuscript

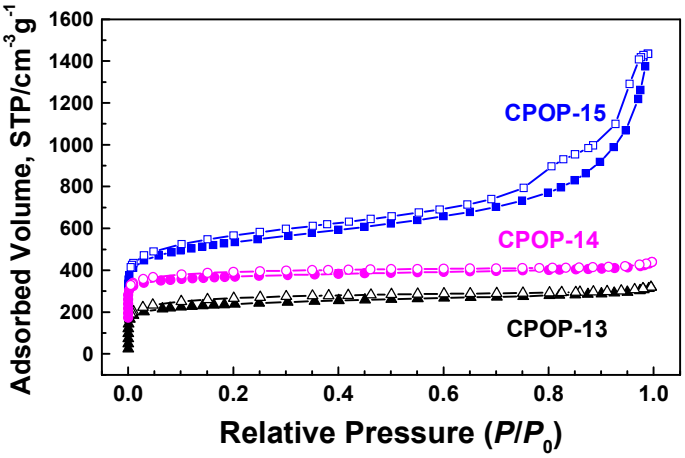


**Fig. 3.** Nitrogen adsorption–desorption isotherms of **CPOP-13**, **CPOP-14**, and **CPOP-15** measured at 77 K. The adsorption and desorption branches are labeled with solid and open symbols, respectively. For clarity, the isotherms of **CPOP-14** and **CPOP-15** were shifted vertically by 150 $cm^3\ g^{-1}$ and 200 $cm^3\ g^{-1}$, respectively.

The porosity parameters of the polymers were investigated by sorption analysis using nitrogen as the sorbate molecule. Nitrogen adsorption–desorption isotherms of CPOPs measured at 77 K are shown in Fig. 3, all obtained samples exhibit a combination of type I and II nitrogen sorption isotherms according to the IUPAC classification.[24] All the nitrogen adsorption–desorption isotherms show rapid uptake at low relative pressure ($P/P_0 = 0–0.1$), indicating the microporous nature. **CPOP-13** and **CPOP-14** possess type I nitrogen gas sorption isotherms and show a very flat sorption plateau. For the polymer **CPOP-15**, the isotherm shows a continuous increase after the adsorption at low relative pressure ($P/P_0 < 0.01$), indicating that an adsorption on the outer surface of small particles in this polymer. Additionally, the increase in the nitrogen sorption at a high relative pressure above 0.9 may arise in part from



Journal of Materials Chemistry A Accepted Manuscript

interparticulate porosity associated with the meso- and macrostructures and interparticular voids of the samples.[25, 26] Furthermore, hysteresis can be observed apparently for all the polymers in the whole range of relative pressure based on the isotherms due to a linear increase of the adsorbed volume upon adsorption, which might be attributed to the swelling in a flexible polymer framework induced by adsorbate molecules dissolved in nominally nonporous parts of the polymer matrix after filling of open and accessible voids or the restricted access of adsorbate to the pores blocked by narrow openings, especially for non-ordered nanoporous materials.[27]

**Table 1.** Porosity Properties and Gas Uptake Capacities of Polymers

| Polymers | $S_{BET}$ [a] ($m^2 g^{-1}$) | $S_{micro}$ [b] ($m^2 g^{-1}$) | $V_{total}$ [c] ($cm^3 g^{-1}$) | $D_{pore}$ [d] (nm) | $CO_2$ uptake [e] (wt.%) | $CH_4$ uptake [e] (wt.%) | $H_2$ uptake [f] (wt.%) |
|---|---|---|---|---|---|---|---|
| **CPOP-13** | 890 | 570 | 0.468 | 0.63, 0.66 | 16.8 | 5.20 | 1.25 |
| **CPOP-14** | 820 | 560 | 0.416 | 0.63, 0.66 | 15.6 | 4.89 | 1.19 |
| **CPOP-15** | 1190 | 330 | 1.575 | 0.63 | 14.2 | 5.39 | 1.29 |

[a] Specific surface area calculated from the nitrogen adsorption isotherm using the BET method; [b] Micropore surface area calculated from the adsorption branch of the nitrogen adsorption−desorption isotherm using the *t*-plot method; [c] Total pore volume at $P/P_0$ = 0.97; [d] Data calculated from nitrogen adsorption isotherms with the NLDFT method; [e] Data were obtained at 1.0 bar and 273 K; [f] Data were obtained at 1.0 bar and 77 K.

Listed in Table 1 are the key porosity properties derived from the isotherm data such as BET specific surface area data, micropore specific surface area data, and pore volumes. The BET specific surface area value was calculated in the relative pressure ($P/P_0$) range from 0.01 to 0.1 according to the previous reports.[28] (Fig. S3, ESI) The



Journal of Materials Chemistry A Accepted Manuscript

BET specific surface area values of **CPOP-13** and **CPOP-14** are 890 and 820 $m^2 g^{-1}$, which is higher than those of **CPOP-2** (510 $m^2 g^{-1}$) and **CPOP-3** (630 $m^2 g^{-1}$)[20] prepared from the same monomer by oxidative coupling reaction, respectively. **CPOP-15** shows a higher BET specific surface area (up to 1180 $m^2 g^{-1}$) than those of the other two materials and can be comparable to the reported hypercrosslinked porous polymers obtained from different coupling polymerization methods.[14, 15] For the non-ordered porous materials, accurate determination of the PSD profile is very difficult, different results are usually obtained according to different approaches. The PSD of the hypercrosslinked porous polymers was calculated from the adsorption branch of the isotherm with the NLDFT approach[29] and exhibited similar PSD profiles as shown in Fig. S4 (ESI). The **CPOP-13** and **CPOP-14** exhibit the similar PSD profile with dominant pore width at 0.63 and 0.66 nm, respectively. For **CPOP-15**, its dominant pore size distribution is only located at 0.63 nm, the monomer possesses more carbazolyl group than that of **CPOP-13** and **CPOP-14,** which means that there are more reaction sites for the oxidative polymerization and Friedel–Crafts reaction. It is reasonable to comprehend that more reaction sites of the monomer result in higher cross-linking structure, which endows the polymers with more stable and permanent pore structure.

The obtained CPOPs with a narrow pore distribution may interact attractively with small gas molecules through improved molecular interaction. Furthermore, electron-rich polycarbazoles network and high charge density at the nitrogen sites of the polymer



Journal of Materials Chemistry A Accepted Manuscript

might facilitate more favorably the interaction between sorbate molecule and adsorbent.[19] On account of the high capacity in gas adsorption for many porous materials, we investigated the uptake capacities of CPOPs for different gas (hydrogen, carbon dioxide, and methane). On the basis of the hydrogen physisorption isotherms measured at 77 K (Fig. S5a, ESI), we found that the hydrogen loading capacity increases with the increase in the specific surface area. The **CPOP-14** possessing the lowest BET specific surface area and total pore volume among the prepared CPOPs exhibits the lowest hydrogen uptake of 1.19 wt% at 1.0 bar and 77 K. **CPOP-15** shows a higher hydrogen uptake of 1.29 wt% at 1.0 bar and 77 K, however, the capacity is moderate and lower than some reported porous polymers such as conjugated porous polymer SPOP-3,[30] triptycene-based porous polymer STP-II,[31] and hypercrosslinked porous polymers.[32] Furthermore, we also investigated the methane uptake capacities of CPOPs according to the similar method (Fig. S5b, ESI), the methane loading capacity also increases with increase in the specific surface area just as the hydrogen uptake capacity. The **CPOP-15** possessing the highest BET specific surface area and total pore volume among the prepared CPOPs exhibits the highest methane uptake of 5.39 wt % at 1.0 bar and 273 K. The methane uptake capacity of **CPOP-15** is not higher than that of the metal–organic framework PCN-14,[33] but better than those of some other porous materials with higher BET specific surface areas such as microporous polycarbazole CPOP-1,[19] MOF $Cu_2$(ebtc), [34] porphyrin-based porous polymer,[21, 35] and adamantane-based porous polymer networks (PPN-2 and PPN-3)[36] under the same



Journal of Materials Chemistry A Accepted Manuscript

conditions. Due to the similar structure of these three polymers, specific surface areas of these CPOPs materials maybe play a key role in the performance of polymers for the methane storage.

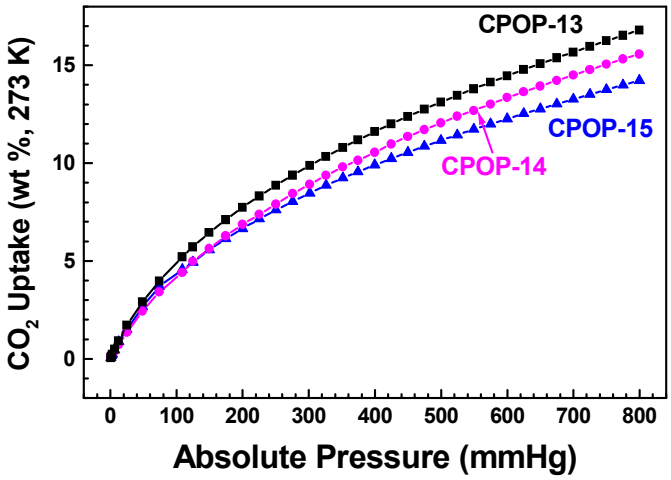


**Fig. 4.** Carbon dioxide adsorption isotherms of the obtained **CPOP-13**, **CPOP-14**, and **CPOP-15** at 273 K.

Furthermore, it should be noticed that the uptake capacity of carbon dioxide is different from those of hydrogen and methane (Table 1). Although **CPOP-15** possesses the highest BET specific surface area and total pore volume, the uptake capacity of carbon dioxide (14.2 wt % at 1.0 bar and 273 K) is the lowest among the prepared CPOPs. For **CPOP-13** and **CPOP-14**, the uptake capacity of carbon dioxide is up to 16.8 and 15.6 wt % at 1.0 bar and 273 K (Fig. 4), which are higher than those of some other porous materials with higher BET specific surface areas under the same conditions.[13, 37, 38] However, their capacities are still moderate when compared with some reported porous polymers with good carbon dioxide uptake capacity, such as



Journal of Materials Chemistry A Accepted Manuscript

polybenzimidazole BILP-1,[39] PAF-1,[40] and PNN-4.[41] The performance could be attributed to the high micropore volume of the polymer and the residual hydroxyl groups in the network. In addition, it is interesting to notice that the uptake capacity of carbon dioxide increases with the increase in the micropore surface area. One common description to explain this experimental result is that the presence of micropore may be beneficial to the carbon dioxide uptake.[37] The gas uptake capacities of the obtained polymers are shown in the Table 1.

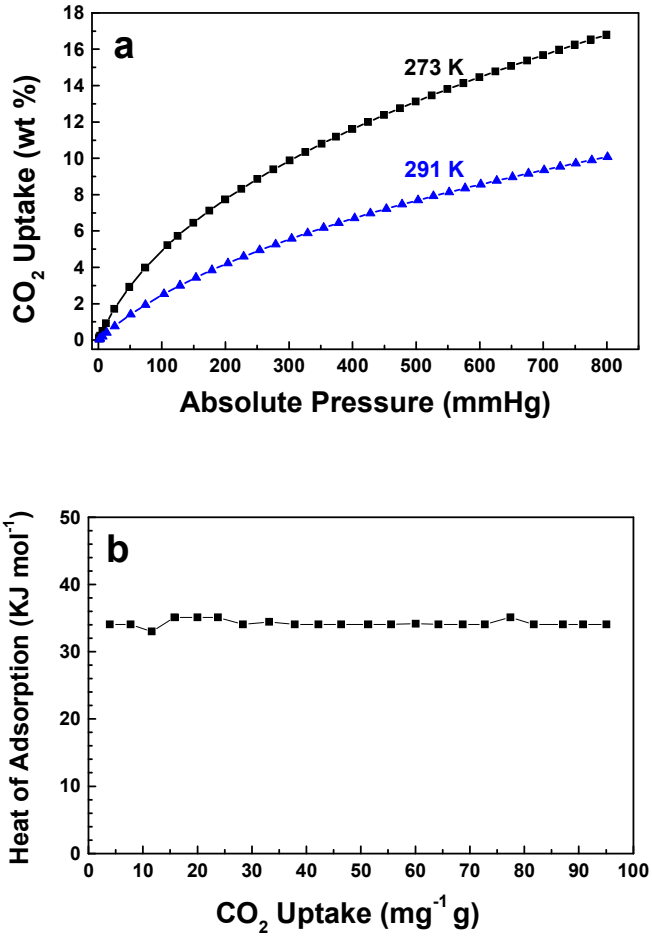


**Fig. 5.** $CO_2$ adsorption isotherms of **CPOP-13** at 273 and 291 K (a) and isosteric heat of $CO_2$ adsorption (b).



Journal of Materials Chemistry A Accepted Manuscript

It is well known that the carbon dioxide uptake capacity for porous polymers can be impacted by the microporosity and the chemical nature of pore surfaces of polymers, in order to further investigate the relationship of carbon dioxide uptake capacity and chemical nature of polymers, we calculated the isosteric heat of carbon dioxide adsorption based on adsorption isotherms at different temperatures (273 and 291 K in the Fig. 5a) through the Clausius−Clapeyron equation.[19, 42] For example, as shown in Fig. 5b, the heat of adsorption of **CPOP-13** for $CO_2$ is up to 34.2 kJ $mol^{-1}$, which is higher than those of **CPOP-14** (32.6 kJ $mol^{-1}$) (Fig. S6, ESI) and **CPOP-15** (32.4 kJ $mol^{-1}$) (Fig. S7, ESI). Most importantly, they remain almost constant over the whole gas loading range. We can find that the heat of adsorption in CPOPs is close to each other, these values are higher than those for other porous polymer analogs, such as HCP materials (20−24 kJ $mol^{-1}$),[14] polybenzimidazole BILP-1 (26.5 kJ $mol^{-1}$),[39] and can be comparable to some CMP materials (25−33 kJ $mol^{-1}$)[43] and polycarbazoles CPOPs (26.5−31.5 kJ $mol^{-1}$).[19, 20] The high adsorption heat for carbon dioxide can be attributed to the affinity to the polarizable $CO_2$ molecules through localdipole/quadrupole interactions, which is facilitated more favorably by electron-rich polycarbazole network and high charge density at the nitrogen sites of polymer.

In addition to the study on the gas (hydrogen, carbon dioxide, and methane) uptake capacity and reversibility of the obtained polymers, it is necessary to investigate the selectivity for different gases, which is very important for potential application in gas separation. Considering the best gas adsorption performance and the highest



Journal of Materials Chemistry A Accepted Manuscript

porosity of **CPOP-1**3 among the obtained polymers, the gas selective adsorption behavior of **CPOP-13** was measured and evidenced by the pure component isotherm data presented in Fig. S8 (ESI). These data show that the carbon dioxide or methane uptake shows a nearly linear increase with the pressure whereas there is no apparent increase trend for nitrogen. The uptake capacities for carbon dioxde (3.8 mmol $g^{-1}$) and methane (3.2 mmol $g^{-1}$) are very close to each other at 273 K and 1.0 bar. In comparison, the nitrogen uptake of **CPOP-13** under the same conditions is only 0.5 mmol $g^{-1}$. We can easily find that CPOP-1 shows significant $CO_2/N_2$ adsorption selectivity. However, the estimated ideal $CO_2/CH_4$ adsorption selectivity is not significant due to the similar saturation capacity.

As we know, the work related to vapor adsorption performance of hypercrosslinked porous polymers is very limited compared with gas adsorption. The porous polymers with high porosity allow potential access by a variety of small molecules. Herein, we also investigated the capability of the obtained CPOPs for adsorption of solvent vapors such as toluene, methanol, and water. We noticed that the three obtained polymers exhibit similar adsorption behavior and toluene is the favorite sorbate molecule. The comparison of vapor adsorption performance for **CPOP-15** is shown in Fig. 6a. Compared with the capacity of water (209 mg $g^{-1}$) and methanol (619 mg $g^{-1}$), the capacity of toluene is highest and up to 1470 mg $g^{-1}$ (about 16.0 mmol $g^{-1}$) at its saturated vapor pressure, the mass ratio of adsorbed water to toluene is up to 1:7, so the obtained CPOPs can be more useful as a kind of hydrophobic material in



Journal of Materials Chemistry A Accepted Manuscript

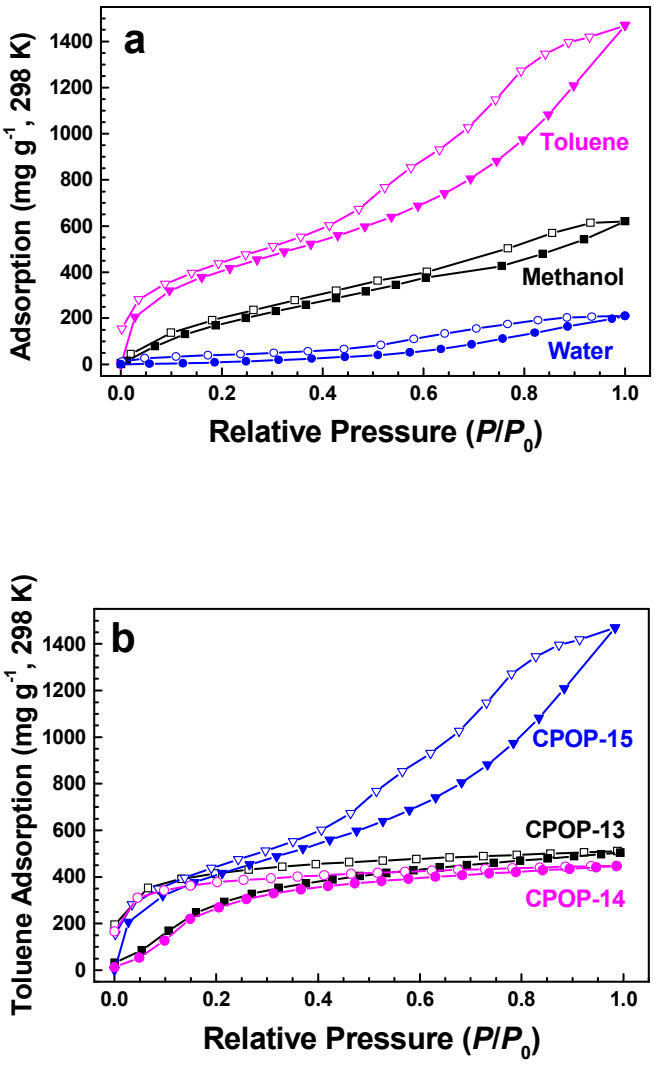


**Fig. 6.** (a) Vapor adsorption isotherms of **CPOP-15** at 298 K and (b) toluene adsorption isotherms of CPOPs at 298 K.

practical applications. One common description to explain this experimental result is that, the obtained polymers are one kind of covalent organic materials that are usually hydrophobic, however, according to polarity of water, methanol and toluene, the hydrophobicity of them decreases in turn. Additionally, the π–π interaction between toluene molecules and the polymers also could be beneficial to the adsorption of



Journal of Materials Chemistry A Accepted Manuscript

polymers for toluene. The vapor adsorption isotherms for the other two polymers are shown in Fig. S9 (ESI). Compared with some reported conjugated porous polymers such as fluorinated porous polymers FPOP-1~2 [44] and hydrophobic porous polymer PAF-11,[45] the higher water uptake of the obtained polymers can be ascribed to the hydroxyl and methoxyl groups produced during the cross-linking reactions.

Toluene adsorption isotherms of the three obtained polymers at 298 K are shown in Fig. 6b. The adsorption of toluene rises gradually until the material reaches saturation, and the adsorption amount of toluene by **CPOP-15** is high up to 1470 mg $g^{-1}$ (about 16.0 mmol $g^{-1}$) at its saturated vapor pressure, which is higher than those of **CPOP-13** (504 mg $g^{-1}$) and **CPOP-14** (447 mg $g^{-1}$) owing to the higher specific surface area. In addition, there is an obvious desorption hysteresis which implies that possible weak host–guest interactions might exist and also indicates the presence of mesopores and capillary condensation. The good sorption capacity of **CPOP-15** for toluene could be ascribed to its high porosities and affinities to the guest molecules including π–π and C–H···π interaction. The adsorption amount of **CPOP-15** for toluene is also higher than those of some reported porous materials such as CPOP-12,[21] FPOP-1,[44] MOF based on a Zinc(II) bipyridine-tetracarboxylate,[46] activated carbon materials,[47] and even higher than PAF-1(1357 mg $g^{-1}$)[40] with ultrahigh specific surface area under the same conditions. Considering the relatively lower specific surface area of 1190 $m^2$ $g^{-1}$, **CPOP-15** exhibits an exceptionally high toluene adsorption capability. This good adsorption performance of **CPOP-15** for toluene would be very promising to eliminate



Journal of Materials Chemistry A Accepted Manuscript

harmful small aromatic molecules in the environment.

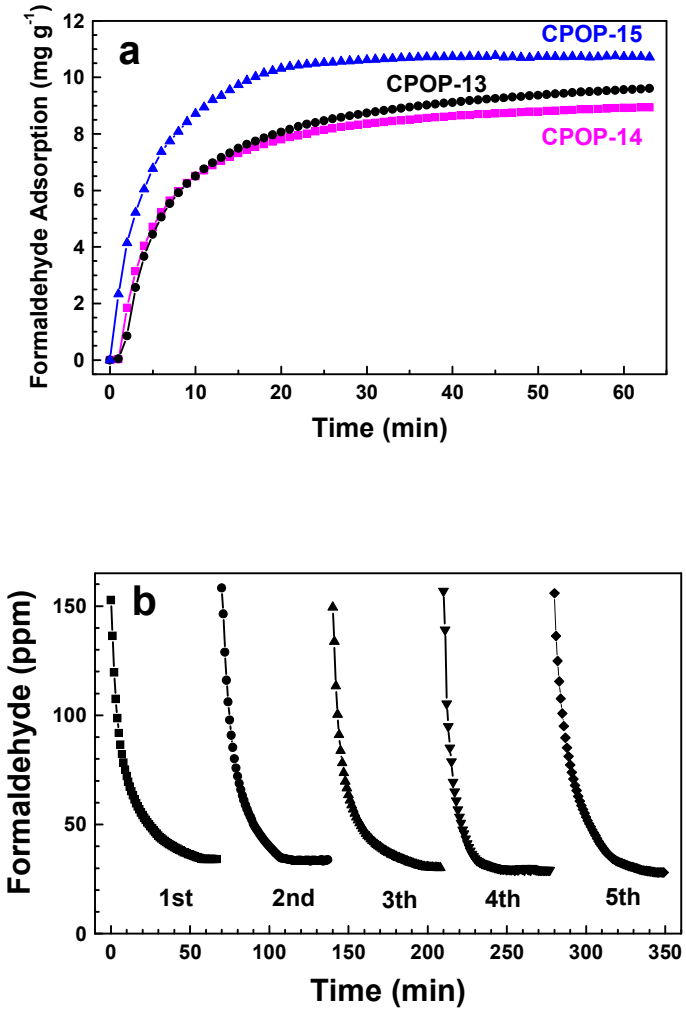


**Fig. 7.** Formaldehyde adsorption isotherms of **CPOP-15** at 298 K (a) and comparison of formaldehyde adsorption with reaction time over 5 times (b).

The indoor air quality is crucial for human health taking into account that people often spend more than 80% of their time in houses, offices, and cars. Volatile organic compounds (VOCs) are among the most abundant indoor air pollutant, formaldehyde (HCHO) is a major pollutant among VOCs.[48, 49] To our best knowledge, the reported



Journal of Materials Chemistry A Accepted Manuscript

work related to formaldehyde adsorption of porous organic polymers is very limited. Polymeric amine-incorporated aminosilicas has been recently reported showing higher formaldehyde adsorption capacity (up to 5.7 mmol $g^{-1}$) than the non-modified silicas.[50] Considering the increasingly indoor air pollution and the high porosity of the porous polymers, we investigated the adsorption capability of CPOPs for formaldehyde. As shown in Fig. 7a, the formaldehyde adsorption of CPOPs is close to each other, **CPOP-15** (10.7 mg $g^{-1}$) is higher than **CPOP-13** (9.6 mg $g^{-1}$) and **CPOP-14** (8.9 mg $g^{-1}$) at ambient temperature and atmosphere, the formaldehyde adsorption on the above adsorbents has positive relationship with the specific surface area of the sample. To further test repeatability of formaldehyde adsorption on the **CPOP-15**, the adsorption experiments were repeatedly performed by five times. In the multiple cycles of adsorption–desorption tests, formaldehyde adsorption was performed at ambient temperature and atmosphere with the initial formaldehyde concentration of ca. 160 ppm for 60 min. After formaldehyde adsorption equilibrium, the formaldehyde was desorbed at 80 °C for 2 h. As shown in Fig. 7b, the **CPOP-15** exhibits relatively good stability and repeatability for formaldehyde adsorption, this is crucial for its practical application. The good performance of CPOPs for formaldehyde adsorption would be very promising to eliminate harmful indoor air pollutant in the environment.

## Conclusions

Considering that both Friedel–Crafts alkylation and carbazole-based oxidative



Journal of Materials Chemistry A Accepted Manuscript

coupling reaction can be catalyzed by $FeCl_3$, a series of hypercrosslinked carbazole-based porous organic polymers via $FeCl_3$-promoted one-step oxidative coupling reaction and Friedel–Crafts alkylation in one pot are reported. The two different reactions can occur simultaneously in the preparative strategy, so more reaction sites can be utilized in the preparation of hypercrosslinked porous polymers, which is beneficial to improve the porosities of polymers, such as the surface area, pore volume, and pore size distribution. The obtained porous polymers with the high BET specific surface area (up to 1190 $m^2 g^{-1}$) show moderate uptake capacities for hydrogen (up to 1.29 wt % at 77 K and 1.0 bar) and carbon dioxide (up to 16.8 wt % at 1.0 bar and 273 K), competitive with the reported results for hypercrosslinked porous polymers under the same conditions. For carbon dioxide adsorption, the heat of adsorption of **CPOP-15** is up to 34.2 kJ $mol^{-1}$, which is higher than those of other porous polymer analogs. Furthermore, the adsorption amount of toluene by **CPOP-15** is high up to 1470 mg $g^{-1}$ (about 16.0 mmol $g^{-1}$) at its saturated vapor pressure; the mass ratio of adsorbed water to toluene is up to 1:7. The hydrophobicity, high porosity, and the π–π interaction between toluene molecules and the polymers could be ascribed to the high adsorption capacity of polymers for toluene. Meanwhile, the obtained CPOPs also possess good formaldehyde adsorption capacity. Especially, **CPOP-15** shows excellent capacities of formaldehyde (up to 10.7 mg $g^{-1}$) at room temperature and atmosphere and exhibits relative good stability and repeatability. In a word, all the outstanding gas adsorption properties make it show potential application to eliminate harmful small molecules in

Journal of Materials Chemistry A Accepted Manuscript

the environment and gas storage and separation in the energy field.

**Acknowledgements.** The financial support of the Ministry of Science and Technology of China (Grant 2014CB932200) and the National Science Foundation of China (Grants no. 21274033, 21374024, and 61261130092) is acknowledged.

**Electronic supplementary information (ESI) available:** Schematic diagram of experimental setup for formaldehyde adsorption, TGA curves, the BET specific surface area plots, pore size distribution, gas (hydrogen and methane) adsorption isotherms, isosteric heat of carbon dioxide adsorption analysis curves, and vapor adsorption isotherms.

**References**

1 P. Kaur, J. T. Hupp, and S. T. Nguyen, Porous organic polymers in catalysis: Opportunities and challenges. *ACS Catal.* **2011**, *1* (7), 819–835.

2 R. Palkovits, M. Antonietti, P. Kuhn, A. Thomas, and F. Schüth, Solid catalysts for the selective low-temperature oxidation of methane to methanol. *Angew. Chem. Int. Ed.* **2009**, *48* (37), 6909–6912.

3 J. Roeser, K. Kailasam; and A. Thomas, Covalent triazine frameworks as heterogeneous catalysts for the synthesis of cyclic and linear carbonates from carbon dioxide and epoxides. *ChemSusChem* **2012**, *5* (9), 1793–1799

4 Y. Zhang and S. N. Riduan, Functional porous organic polymers for heterogeneous catalysis. *Chem. Soc. Rev.* **2012**, *41* (6), 2083–2094.



Journal of Materials Chemistry A Accepted Manuscript

5 J. Germain, J. M. J. Fréchet, and F. Svec, Nanoporous polymers for hydrogen storage. *Small* **2009**, *5* (10), 1098–1111.

6 R. Dawson, A. I. Cooper, and D. J. Adams, Nanoporous organic polymer networks. *Progress in Polymer Science* **2012**, *37* (4), 530–563.

7 C. G. Bezzu, M. Carta, A. Tonkins, J. C. Jansen, P. Bernardo, F. Bazzarelli, and N. B McKeown, A spirobifluorene-based polymer of intrinsic microporosity with improved performance for gas separation. *Adv. Mater.* **2012**, *24* (44), 5930–5933.

8 N. Du, H. B. Park, G. P. Robertson, M. M. Dal-Cin, T. Visser, L. Scoles, and M. D. Guiver, Polymer nanosieve membranes for $CO_2$-capture applications. *Nat. Mater.* **2011**, *10* (5), 372–375.

9 N. B. McKeown and P. M. Budd, Exploitation of intrinsic microporosity in polymer-based materials. *Macromolecules* **2010**, *43* (12), 5163–5176.

10 J.-X. Jiang and A. I Cooper, Microporous organic polymers: Design, synthesis, and function. in *Topics in Current Chemistry. 293. Functional Metal–Organic Frameworks: Gas Storage, Separation and Catalysis*, Schröder, M., Ed. Springer Berlin Heidelberg. **2010**, pp 1–33.

11 S. Ren, M. J. Bojdys, R. Dawson, A. Laybourn, Y. Z. Khimyak, D. J. Adams, and A. I. Cooper, Porous, fluorescent, covalent triazine-based frameworks via room-temperature and microwave-assisted synthesis. *Adv. Mater.* **2012**, *24* (17), 2357–2361.

12 D. Wu, F. Xu, B. Sun, R. Fu, H. He, and K. Matyjaszewski, Design and preparation of porous polymers. *Chem. Rev.* **2012**, *112* (7), 3959–4015.

13 C. F. Martin, E. Stockel, R. Clowes, D. J. Adams, A. I. Cooper, J. J. Pis, F. Rubiera, and C. Pevida, Hypercrosslinked organic polymer networks as potential adsorbents for pre-combustion $CO_2$ capture. *J. Mater. Chem.* **2011**, *21* (14), 5475–5483.

14 S. Xu, Y. Luo, and B. Tan, Recent development of hypercrosslinked microporous organic polymers. *Macromol. Rapid Commun.* **2013**, *34* (6), 471–484.

15 Y. Luo, B. Li, W. Wang, K. Wu, and B. Tan, Hypercrosslinked aromatic heterocyclic

Journal of Materials Chemistry A Accepted Manuscript

microporous polymers: A new class of highly selective $CO_2$ capturing materials. *Adv. Mater.* **2012**, *24* (42), 5703–5707.

16 Y. Luo, S. Zhang, Y. Ma, W. Wang, and B. Tan, Microporous organic polymers synthesized by self-condensation of aromatic hydroxymethyl monomers. *Polym. Chem.* **2013**, *4* (4), 1126–1131.

17 B. Li, R. Gong, W. Wang, X. Huang, W. Zhang, H. Li, C. Hu, and B. Tan, A new strategy to microporous polymers: Knitting rigid aromatic building blocks by external cross-linker. *Macromolecules* **2011**, *44* (8), 2410–2414.

18 , D. S. Kundu, J. Schmidt, C. Bleschke, A. Thomas, and S. Blechert, A microporous binol-derived phosphoric acid. *Angew. Chem. Int. Ed.* **2012**, *51* (22), 5456–5459.

19 Q. Chen, M. Luo, P. Hammershoj, D. Zhou, Y. Han, B. W. Laursen, C.-G. Yan, and B.-H. Han, Microporous polycarbazole with high specific surface area for gas storage and separation. *J. Am. Chem. Soc.* **2012**, *134* (14), 6084–6087.

20 Q. Chen, D.-P. Liu, M. Luo, L.-J. Feng, Y.-C. Zhao, and B.-H. Han, Nitrogen-containing microporous conjugated polymers via carbazole-based oxidative coupling polymerization: Preparation, porosity, and gas uptake. *Small* **2014**, *10* (2), 308–315.

21 L.-J. Feng, Q. Chen, J.-H. Zhu, D.-P. Liu, Y.-C. Zhao, and B.-H. Han, Adsorption performance and catalytic activity of porous conjugated polyporphyrins via carbazole-based oxidative coupling polymerization. *Polym. Chem.* **2014**, *5* (8), 3081–3088.

22 Y. Le, D. Guo, B. Cheng, and J. Yu, Bio-template-assisted synthesis of hierarchically hollow $SiO_2$ microtubes and their enhanced formaldehyde adsorption performance. *Appl. Surface Sci.* **2013**, *274*, 110–116.

23 N. Fontanals, J. Cortés, M. Galià, R. Maria Marcé, P. A. G. Cormack, F. Borrull, and D. C. Sherrington, Synthesis of Davankov-type hypercrosslinked resins using different isomer compositions of vinylbenzyl chloride monomer, and application in the solid-phase extraction of polar compounds. *Polym. Chem.* **2005**, *43* (8), 1718–1728.

Journal of Materials Chemistry A Accepted Manuscript

24 K. S. W. Sing, D. H. E., R. A. W. Haul, L. Moscou, R. A. Pierotti, J. Rouquérol and T. Siemieniewska, Reporting physisorption data for gas/solid systems with special reference to the determination of surface area and porosity. *Pure Appl. Chem.* **1985**, *57* (4), 603–619.

25 Q. Chen, M. Luo, T. Wang, J.-X. Wang, D. Zhou, Y. Han, C.-S. Zhang, C.-G. Yan, and B.-H. Han, Porous organic polymers based on propeller-like hexaphenylbenzene building units. *Macromolecules* **2011**, *44* (14), 5573-5577.

26 M. Rose, N. Klein, W. Bohlmann, B. Bohringer, S. Fichtner, and S. Kaskel, New element organic frameworks via Suzuki coupling with high adsorption capacity for hydrophobic molecules. *Soft Matter.* **2010**, *6* (16), 3918–3923.

27 M. Rose, W. Bohlmann, M. Sabo, and S. Kaskel, Element-organic frameworks with high permanent porosity. *Chem. Commun*. **2008**, (21), 2462–2464.

28 K. S. Walton and R. Q. Snurr, Applicability of the BET method for determining surface areas of microporous metal−organic frameworks. *J. Am. Chem. Soc.* **2007**, *129* (27), 8552–8556.

29 J. Weber, J. Schmidt, A. Thomas, and W. Bohlmann, Micropore analysis of polymer networks by gas sorption and $^{129}$Xe NMR spectroscopy: Toward a better understanding of intrinsic microporosity. *Langmuir* **2010**, *26* (19), 15650–15656.

30 Q. Chen, J.-X. Wang, Q. Wang, N. Bian, Z.-H. Li, and B.-H. Han, Spiro(fluorene-9,9'-xanthene)-based porous organic polymers: preparation, porosity and exceptional hydrogen uptake at low pressure. *Macromolecules*, **2011**, *44* (20), 7987–7993.

31 C. Zhang, Y. Liu, B. Li, B. Tan, C.-F. Chen, H.-B. Xu, and X.-L. Yang, Triptycene-based microporous polymers: synthesis and their gas storage properties. *ACS Macro Lett.* **2012**, *1* (1), 190–193.

32 J. Germain, J. M. J. Frechét, and F. Svec, Nanoporous polymers for hydrogen storage. *Small* **2009**, *5* (10), 1098–1111.

33 S. Ma, D. Sun, J. M. Simmons, C. D. Collier, D. Yuan, and H.-C. Zhou, Metal-organic framework from an anthracene derivative containing nanoscopic cages

Journal of Materials Chemistry A Accepted Manuscript

exhibiting high methane uptake. *J. Am. Chem. Soc.* **2008**, *130* (3), 1012−1016.

34 Y. Hu, S. Xiang, W. Zhang, Z. Zhang, L. Wang, J. Bai, and B. Chen, A new MOF-505 analog exhibiting high acetylene storage. *Chem. Commun*. **2009**, (48), 7551−7553.

35 Z. Wang, S. Yuan, A. Mason, B. Reprogle, D.-J. Liu, and L. Yu, Nanoporous porphyrin polymers for gas storage and separation. *Macromolecules* **2012**, *45* (18), 7413−7419.

36 W. Lu, D. Yuan, D. Zhao, C. I. Schilling, O. Plietzsch, T. Muller, S. Bräse, J. Guenther, J. Blümel, R. Krishna, Z. Li, and H.-C. Zhou, Porous polymer networks: synthesis, porosity, and applications in gas storage/separation. *Chem. Mater.* **2010**, *22* (21), 5964−5972.

37 O. K. Farha, Y. -S. Bae, B. G. Hauser, A. M. Spokoyny, R. Q. Snurr, C. A. Mirkin, and J. T. Hupp, Chemical reduction of a diimide based porous polymer for selective uptake of carbon dioxide versus methane. *Chem. Commun.* **2010**, *46* (7), 1056−1058.

38 O. K. Farha, A. M. Spokoyny, B. G. Hauser, Y. S. Bae, S. E. Brown, R. Q. Snurr, C. A. Mirkin, and J. T. Hupp, Synthesis, properties, and gas separation studies of a robust diimide-based microporous organic polymer. *Chem. Mater.* **2009**, *21* (14), 3033−3035.

39 M. G. Abbani and H. M. El-Kaderi, Template-free synthesis of a highly porous benzimidazole-linked polymer for $CO_2$ capture and $H_2$ storage. *Chem. Mater.* **2011**, *23* (7), 1650−1653.

40 T. Ben, H. Rao, S. Ma, D. Cao, J. Lan, X. Jing, W. Wang, J. Xu, F. Deng, J. M. Simmons, S. Qui, and G. Zhu, Targeted synthesis of a porous aromatic framework with high stability and exceptionally high surface area. *Angew. Chem., Int. Ed.* **2009**, *48* (50), 9457–9460.

41 D. Yuan, W. Lu, D. Zhao, and H.-C. Zhou, Highly stable porous polymer networks with exceptionally high gas-uptake capacities. *Adv. Mater.* **2011**, *23* (32), 3723–3725.

42 J. A. Dunne, M. Rao, S. Sircar, R. J. Gorte, and A. L. Myers, Calorimetric heats of adsorption and adsorption isotherms. 2. $O_2$, $N_2$, Ar, $CO_2$, $CH_4$, $C_2H_6$, and $SF_6$ on NaX, H-ZSM-5, and Na-ZSM-5 zeolites. *Langmuir* **1996**, *12* (24), 5896–5904.

Journal of Materials Chemistry A Accepted Manuscript

43 R. Dawson, D. J. Adams, and A. I. Cooper, Chemical tuning of $CO_2$ sorption in robust nanoporous organic polymers. *Chem. Sci.* **2011**, *2* (6), 1173–1177.

44 D.-P. Liu, Q. Chen, Y.-C. Zhao, L.-M. Zhang, A. D. Qi, and B.-H. Han, Fluorinated porous organic polymers via direct C–H arylation polycondensation. *ACS Macro Lett.* **2013**, *2* (6), 522–526.

45 Y. Yuan, F. Sun, H. Ren, X. Jing, W. Wang, H. Ma, H. Zhao, and G. Zhu, Targeted synthesis of a porous aromatic framework with a high adsorption capacity for organic molecules. *J. Mater. Chem.* **2011**, *21* (35), 13498–13502.

46 X. Lin, A. J. Blake, C. Wilson, X. Z. Sun, N. R. Champness, M. W. George, P. Hubberstey, R. Mokaya, and M. A. Schroder, Porous framework polymer based on a zinc(ii) 4,4'-bipyridine-2,6,2',6'-tetracarboxylate: Synthesis, structure, and "zeolite-like" behaviors. *J. Am. Chem. Soc.* **2006**, *128* (33), 10745–10753.

47 L. Luo, D. Ramirez, M. Rood, G. Grevillot, K. James Hay, and D. Thurston, Adsorption and electrothermal desorption of organic vapors using activated carbon adsorbents with novel morphologies. *Carbon* **2006**, *44* (13), 2715–2723.

48 J. J. Collins, R. Ness, R. W. Tyl, N. Krivanek, N. A. Esmen, and T. A. Hall, A review of adverse pregnancy outcomes and formaldehyde exposure in human and animal studies. *Regulatory Toxicology and Pharmacology* **2001**, *34* (1), 17–34.

49 L. Nie, J. Yu, X. Li, B. Cheng, G. Liu, and M. Jaroniec, Enhanced performance of naoh-modified pt/tio$_2$ toward room temperature selective oxidation of formaldehyde. *Environ. Sci. Technol.* **2013**, *47* (6), 2777–2783.

50 A. Nomura, and C. W. Jones, Enhanced formaldehyde-vapor adsorption capacity of polymeric amine-incorporated aminosilicas. *Chem. Eur. J.* **2014**, *20* (21), 6381–6390.

Journal of Materials Chemistry A Accepted Manuscript

## Table of Contents/Abstract Graphic

Hypercrosslinked carbazole-based porous organic polymers were prepared via $FeCl_3$-promoted one-step oxidative coupling reaction and Friedel–Crafts alkylation in one pot.

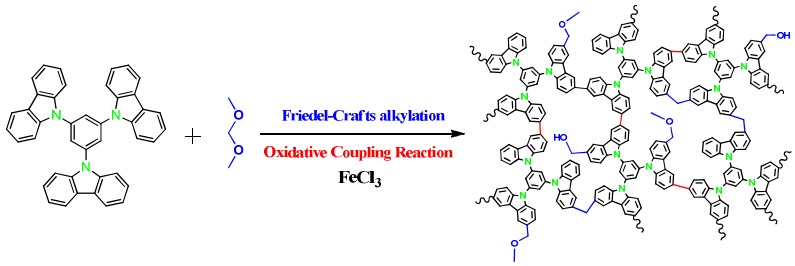


Journal of Materials Chemistry A Accepted Manuscript